

6-1-2011

BRANCHLESS TRICHOMES links cell shape and cell cycle control in *Arabidopsis* trichomes

Remmy Kasili
Louisiana State University

Cho Chun Huang
University of Cologne

Jason D. Walker
Louisiana State University

L. Alice Simmons
Louisiana State University

Jing Zhou
Louisiana State University

See next page for additional authors

Follow this and additional works at: https://digitalcommons.lsu.edu/biosci_pubs

Recommended Citation

Kasili, R., Huang, C., Walker, J., Simmons, L., Zhou, J., Faulk, C., Hülskamp, M., & Larkin, J. (2011). BRANCHLESS TRICHOMES links cell shape and cell cycle control in *Arabidopsis* trichomes. *Development*, 138 (11), 2379-2388. <https://doi.org/10.1242/dev.058982>

This Article is brought to you for free and open access by the Department of Biological Sciences at LSU Digital Commons. It has been accepted for inclusion in Faculty Publications by an authorized administrator of LSU Digital Commons. For more information, please contact ir@lsu.edu.

Authors

Remmy Kasili, Cho Chun Huang, Jason D. Walker, L. Alice Simmons, Jing Zhou, Chris Faulk, Martin Hülkamp, and John C. Larkin

BRANCHLESS TRICHOMES links cell shape and cell cycle control in *Arabidopsis* trichomes

Remmy Kasili^{1,*†}, Cho-Chun Huang^{2,†,‡}, Jason D. Walker^{1,§}, L. Alice Simmons¹, Jing Zhou^{1,¶}, Chris Faulk¹, Martin Hülskamp² and John C. Larkin^{1,**}

SUMMARY

Endoreplication, also called endoreduplication, is a modified cell cycle in which DNA is repeatedly replicated without subsequent cell division. Endoreplication is often associated with increased cell size and specialized cell shapes, but the mechanism coordinating DNA content with shape and size remains obscure. Here we identify the product of the *BRANCHLESS TRICHOMES* (*BLT*) gene, a protein of hitherto unknown function that has been conserved throughout angiosperm evolution, as a link in coordinating cell shape and nuclear DNA content in endoreplicated *Arabidopsis* trichomes. Loss-of-function mutations in *BLT* were found to enhance the multicellular trichome phenotype of mutants in the *SIAMESE* (*SIM*) gene, which encodes a repressor of endoreplication. Epistasis and overexpression experiments revealed that *BLT* encodes a key regulator of trichome branching. Additional experiments showed that *BLT* interacts both genetically and physically with *STICHEL*, another key regulator of trichome branching. Although *b/t* mutants have normal trichome DNA content, overexpression of *BLT* results in an additional round of endoreplication, and *b/t* mutants uncouple DNA content from morphogenesis in mutants with increased trichome branching, further emphasizing its role in linking cell shape and endoreplication.

KEY WORDS: *Arabidopsis*, Cell cycle, Endoreduplication, Endoreplication, Trichome

INTRODUCTION

The acquisition of plant form requires the development of multiple cell types from meristematic cells to form the tissues and organs that make up the mature plant. These diverse cell types must not only be arranged in the correct spatial pattern but also take the correct shape. Indeed, much of plant growth involves the directionally controlled expansion of cells, as opposed to cell proliferation. The cytoskeleton plays an important role in determining plant cell shape by influencing the pattern in which cell wall materials are deposited in expanding cells (Smith and Oppenheimer, 2005; Szymanski, 2009). Cell expansion is achieved by the cell wall yielding to turgor pressure from within, the resultant breakage and reformation of bonds between cell wall components and the controlled deposition of new wall materials (Szymanski and Cosgrove, 2009). The determinants of the polarity of cell expansion remain unclear, although recent work has implicated interactions between Rho family GTPases and cytoskeletal components (Yang, 2008; Szymanski, 2009).

Cell differentiation is also often accompanied by alterations in the cell cycle. These modifications range from simple arrest of the cell cycle in the differentiating cell to patterns of stereotyped

cell divisions, as are seen in stomatal and root development (Verkest et al., 2005b; Abrash and Bergmann, 2009). One type of altered cell cycle that is commonly seen in large or metabolically active differentiated cells is endoreplication, also known as endoreduplication (Vlieghe et al., 2007). This modified cell cycle involves repeated replication of nuclear DNA without subsequent cell division. The DNA content of endoreplicated cells is typically correlated with cell size (Melaragno et al., 1993; Hülskamp et al., 1994). Although we are beginning to understand the alterations in the plant cell cycle that result in endoreplication (Vlieghe et al., 2007), essentially nothing is known of the mechanisms that coordinate DNA content and cell size in an endoreplicated cell.

Arabidopsis trichomes (shoot epidermal hairs) are large specialized single cells that project from the epidermis of leaves, petioles, sepals and stems. Trichomes have a unique branched cellular architecture; on leaves, they typically have three or four branches (Schellmann and Hülskamp, 2005). *Arabidopsis* trichomes are well established as a system for studying cell fate determination, cell morphogenesis and endoreplication (Larkin et al., 2007; Pesch and Hülskamp, 2009; Szymanski, 2009). The initiation of trichome development on *Arabidopsis* leaves is promoted by a transcription factor complex consisting of the bHLH transcription factors GL3 and EGL3, the Myb transcription factors GL1 and MYB23 and the WD-repeat protein TTG. Selection of trichome precursor cells depends on cell-to-cell movement of both the positive regulator TTG and the negative transcriptional regulator TRY and related proteins (Bouyer et al., 2008). One of the earliest events in trichome development is the initiation of endoreplication, and the developing trichome typically undergoes three to four rounds of DNA replication without division during its development (Hülskamp et al., 1994). The developing trichome cell then expands from the plane of the epidermis and typically undergoes two to three branching events, resulting in a total of three to four branches in the mature trichome (Szymanski, 2009).

¹Department of Biological Sciences, Louisiana State University, Baton Rouge, LA 70803-1715, USA. ²Botanical Institute, University of Cologne, Gyrhofstrasse 15, 50931 Cologne, Germany.

*Present address: National Institute of Child Health and Human Development, Bethesda, MD 20892, USA

†These authors contributed equally to this work

‡Present address: Department of Forest Genetics, Umeå Plant Science Centre, Swedish University of Agricultural Sciences, S-90183 Umeå, Sweden

§Present address: Department of Pathobiological Sciences, LSU School of Veterinary Medicine, Louisiana State University, Baton Rouge, LA 70803, USA

¶Present address: LSU School of Medicine, Louisiana State University Health Sciences Center, New Orleans, LA 70112, USA

**Author for correspondence (jlarkin@lsu.edu)

The final phase of expansion is driven by enlargement of the trichome vacuole, and development concludes with maturation of the thick cellulose cell wall.

Mutations in a number of genes are known to affect endoreplication levels in trichomes (for a review, see Larkin et al., 2007). These include cell cycle components that affect the G1/S transition and DNA replication such as *RBR* (Desvoyes et al., 2006) and *CDC6* (Castellano et al., 2004), and transcriptional regulators of trichome cell fate, such as *GL3* and *TRY* (Hülkamp et al., 1994). In general, mutations in genes that increase or decrease the number of rounds of endoreplication increase or decrease, respectively, trichome cell size and the number of branches. Because both of these classes of genes encode proteins involved in nuclear processes, they presumably influence cell size and branch initiation indirectly. However, essentially nothing is known of the mechanism that coordinates endoreplication with cell size and shape.

Mutations affecting trichome branching and cell shape that do not affect endoreplication are also known (Schellmann and Hülkamp, 2005), and these presumably include factors that function primarily in branch initiation and expansion. The mechanism for polarizing branch initiation sites is not understood, but recent work has focused on two proteins. Recessive loss-of-function mutations in *STICHEL* (*STI*), which encodes a protein with sequence similarity to eubacterial DNA polymerase III γ -subunits (Ilgenfritz et al., 2003), and *BRANCHLESS TRICHOMES* (*BLT*), which encodes a protein with no similarity to proteins of known function, both result in trichomes that are completely unbranched. Recently, both of these proteins were localized to newly initiated trichome branch points (Marks et al., 2009), indicating that *STI* and *BLT* are excellent candidates for proteins that determine branch sites. Mutations in *STI* appear to have no effect on endoreplication (Ilgenfritz et al., 2003), and the effect of *BLT* on endoreplication has not been investigated previously.

The recessive *siamese* (*sim*) mutation results in multicellular trichomes in place of the unicellular trichomes of wild-type plants (Walker et al., 2000). The *SIM* gene encodes a cyclin-dependent kinase inhibitor that is a regulator of endoreplication onset during trichome cell differentiation (Churchman et al., 2006). Here, we report the isolation of a *blt* mutation based on its genetic enhancement of the *sim* multicellular trichome phenotype, and show that *BLT*, a major regulator of trichome branch initiation, also regulates endoreplication levels. In addition to its effects on the cell cycle, we show that *BLT* protein interacts directly with *STI* in the regulation of branching. This work suggests that *BLT*, a key regulator of trichome cell shape, also plays a role in integrating endoreplication levels with cell shape.

MATERIALS AND METHODS

Plant material and growth conditions

Plants were grown as previously described (Larkin et al., 1999). The loss-of-function *blt* insertion line SAIL_632_G06.V1 (Columbia ecotype) was obtained from the Arabidopsis Biological Resource Center. The origin of the *sim-1* allele used for mutagenesis has been described previously (Churchman et al., 2006). The *try-JC* allele has also been described previously (Larkin et al., 1999; Schellmann et al., 2002); in the work of Schellman et al. (Schellman et al., 2002), which describes the molecular defect, it is mislabeled as the *try-5C* allele. The *nok-122* and *kak-2* alleles (Hülkamp et al., 1994; Folkers et al., 1997) and the *GL2pro:GL3* line (Kirik et al., 2001) have been described previously. The *rfi* allele (Perazza et al., 1999) was obtained from Jean-Marc Bonneville. The *gl3-sst* allele (Esch et al., 2003) was obtained from M. David Marks. The ethyl methane sulfonate (EMS)-induced *sti-AS* allele was obtained from Alan Sessions

(University of California, Berkeley). All alleles were either generated in Col-0, or were backcrossed three times to Col-0 before selfing to obtain homozygotes. Putative double mutants were confirmed by complementation, by crossing to wild-type plants and recovering the two parental mutant phenotypes in a segregating F2, or by sequencing.

Isolation of the *blt-3* allele

As described previously (Kasili et al., 2010), homozygous seeds of *sim-1* were mutagenized with EMS and collected as 37 pools of 300 M₁ plants (a total of 11,100 M₁ plants) and ~2000 M₂ plants per pool were screened for *sim* phenotypic modifiers. Plants exhibiting increased multicellularity and clustering of trichomes were selfed. These putative modifiers were then backcrossed three times to the *sim-1* mutant, and plants having the enhanced *sim* phenotype were selected for further work. The presumed double mutants were crossed to Col-0 wild type and the F1 selfed to isolate the modifier as a single mutant. Plants with reduced trichome branching but no multicellular trichomes or trichome clusters were observed in this segregating population. This phenotype segregated as a recessive monogenic trait, and when the new mutant was crossed to either the *sim-1* or *sim-2* alleles it reconstructed the enhanced multicellularity of the original isolate, confirming that this mutant was the *sim* modifier of interest.

Genetic mapping and identification of *BLT* as the genetic modifier

Using bulked segregant analysis (Lukowitz et al., 2000), the reduced trichome branching phenotype of the modifier was mapped to a region on chromosome I. Genomic DNA from 971 plants from an F2 population of a cross between the mutant (in Col-0) and Landsberg *erecta* (*Ler*) was genotyped by PCR with molecular markers generated using the Cereon database of the Columbia and *Ler* polymorphisms at TAIR (<http://www.arabidopsis.org/browse/Cereon/index.jsp>). Two restriction enzyme-cleavable PCR-amplifiable markers, F13O11-4 and F1N19-7, were used to localize the mutation within a region of ~70 kb on two overlapping BAC clones, F1N19 and F13O11. Sequencing genes within this region revealed a G-to-A point mutation in the gene *AT1G64690*. This gene is known as *BRANCHLESS TRICHOMES*, and loss-of-function *blt* mutations reduce trichome branching (Marks et al., 2009). The EMS-induced allele described here was designated *blt-3* in accordance with the naming of previously published alleles.

For molecular complementation, the genomic coding sequence of *AT1G64690*, together with 1447 bp of upstream sequence and 1228 bp of downstream sequence, was PCR amplified from the BAC clone F1N19 using primers ENS1CF (5'-CACCTGTGACAGACTTGCTCCTAC-3') and ENS1CR2 (5'-CAGCCACATAAGGACCCGAC-3'). This fragment was cloned into the Gateway pENTR vector following the manufacturer's protocol (Invitrogen, Carlsbad, CA, USA). Error-free entry clones were confirmed by sequence analysis before attL recombination into the Gateway destination vector pMDC100, a plant binary transformation vector, to create pMDC100/ENS1C-3.5, which was then used for transformation of homozygous *blt-3* plants.

Phylogenetic analysis of *BLT*-related gene families

Predicted protein sequences for *BLT*, *At1G50660*, *At5g22310*, *At3g11590* and *At3g20350* were obtained from TAIR (<http://www.arabidopsis.org>) and used in NCBI BLAST searches with the TBLASTN option. The most similar predicted protein sequence to each of the five query sequences in the genomes of *Arabidopsis lyrata* (L.) O'Kane & Al-Shehbaz, *Vitis vinifera* (L.), *Ricinus communis* (L.) and *Populus trichocarpa* (Torr. & A.Gray) and *Sorghum bicolor* (L.) Moench was retained for analysis. Including the five query sequences, this resulted in 24 protein sequences, predicted from the following GenBank accession numbers: *A. thaliana* *BLT*, NM_105144; *A. lyrata* *BLT*, XM_002887821; *R. communis* *BLT*, XM_002518874; *P. trichocarpa* *BLT*, XM_002297906; *V. vinifera* *BLT*, XM_002272534; *S. bicolor* *BLT*, XM_002467436; *At1G50660*, NM_103948; *At5g22310*, NM_122136; *At3g11590*, NM_101041; *At3g20350*, NM_112926; *A. lyrata-2*, XM_002891541; *A. lyrata-3*, XM_002874015; *A. lyrata-4*, XM_002882692; *R. communis-2*, XM_002532506; *R. communis-3*, XM_002523807; *R. communis-4*, XM_002530473; *P. trichocarpa-2*, XM_002316730; *P. trichocarpa-3*, XM_002328072; *P. trichocarpa-4*, XM_002309373; *V. vinifera-2*

XM_002280300; *V. vinifera*-3, XM_002275870; *S. bicolor*-2, XM_002448513; *S. bicolor*-3, XM_002441284; and *S. bicolor*-4, XM_002447617.

Alignment of these 24 predicted protein sequences was performed using Mega4 (MEGA Software) using the ClustalW algorithm with default parameters (multiple alignment gap opening penalty=10; gap extension penalty=0.2; Gonnet matrix, residue-specific penalties, on; hydrophilic penalties, on; gap separation distance=4; end gap separation, off; use negative matrix, off; delay divergent cut-off %=30). The phylogeny was built in Mega4 using neighbor joining with 1000 bootstrap iterations. The resulting tree was arbitrarily rooted between the BLT subfamily and all other paralogs. For the alignment used to produce this tree, see Fig. S3 in the supplementary data,

Generation of transgenic lines

The full-length *BLT* coding region was PCR amplified from the BAC clone FIN19 using primers ENSIF (5'-CACCATGAAGGATATGAAGA-TGCAGAGC-3') and ENSIR1 (5'-TCAAGGAGGAGGAGAGGAGAGA-3'), which contains a stop codon, or ENSIR2 (5'-AGGAGGAGGAGGAGGAGAGAAGAG-3'), which lacks a stop codon, and cloned into the Gateway vector pENTR following the manufacturer's protocol (Invitrogen). Error-free entry clones were confirmed by DNA sequencing before attL recombination into the Gateway-compatible destination binary vector pLEELA-pGL2 (Weinl et al., 2005) for overexpression in developing trichomes. The resulting plasmids were introduced into *Agrobacterium tumefaciens* by electroporation or by the freeze-thaw method (Weigel and Glazebrook, 2002) and subsequently introduced into plants by the floral dip method (Clough and Bent, 1998). Transgenic plants were selected on MS medium containing the relevant antibiotics and then transferred to soil.

Microscopy

The in situ DNA content of trichomes was measured as described (Walker et al., 2000), and the DNA values were normalized to reported wild-type epidermal cell nuclei values (Melaragno et al., 1993). Statistical analysis was performed using SigmaStat (Systat Software, San Jose, CA, USA). Flow cytometry was performed as described (Verkest et al., 2005a).

Trichomes were examined using scanning electron microscopy (SEM) as previously described (Larkin et al., 1999). Trichome branches were counted on all trichomes on the adaxial side of the first or second leaf from at least ten plants of each genotype.

Yeast two-hybrid and bimolecular fluorescence complementation protein-protein interaction assays

Entry clones containing full-length cDNA of *BLT* or *STI* or a cDNA fragment of *STI* (encoding the N-terminal 454 amino acids) were transferred to the Gateway-compatible yeast two-hybrid vectors pAS-attR and pACT-attR by LR recombination following the manufacturer's protocol (Invitrogen) and used to transform yeast strain AH109. Assays for α -galactosidase activity resulting from expression of the GAL4-responsive *MEL1* gene present in the AH109 host strain were conducted as described in the Clontech Yeast Protocols Handbook (PR973283, July 2009). Six transformed colonies were analyzed per genotype. Results are reported in milliunits (mU) of α -galactosidase activity $\text{ml}^{-1} \text{cell}^{-1}$; one unit of α -galactosidase activity is defined as the amount of enzyme that hydrolyzes 1 μmole p-nitrophenyl- α -D-galactoside to p-nitrophenol and D-galactose in 1 minute at 30°C in acetate buffer (pH 4.5) (Aho et al., 1997).

For bimolecular fluorescence complementation (BiFC), entry clones of full-length *BLT* and *STI* were fused with the C-terminal and N-terminal split fragments of YFP, respectively, in the BiFC pBatTL vectors (Uhrig et al., 2007) by Gateway recombination, and were introduced into onion cells by biolistic bombardment.

RESULTS

Identification of *blt* as a genetic enhancer of the *sim* multicellular trichome phenotype

siamese-1 (*sim-1*) is a loss-of-function mutation that results in multicellular trichomes that occur in clusters (Fig. 1A,B; Table 1). *SIM* encodes a CDK inhibitor that binds to CYCD-CDK

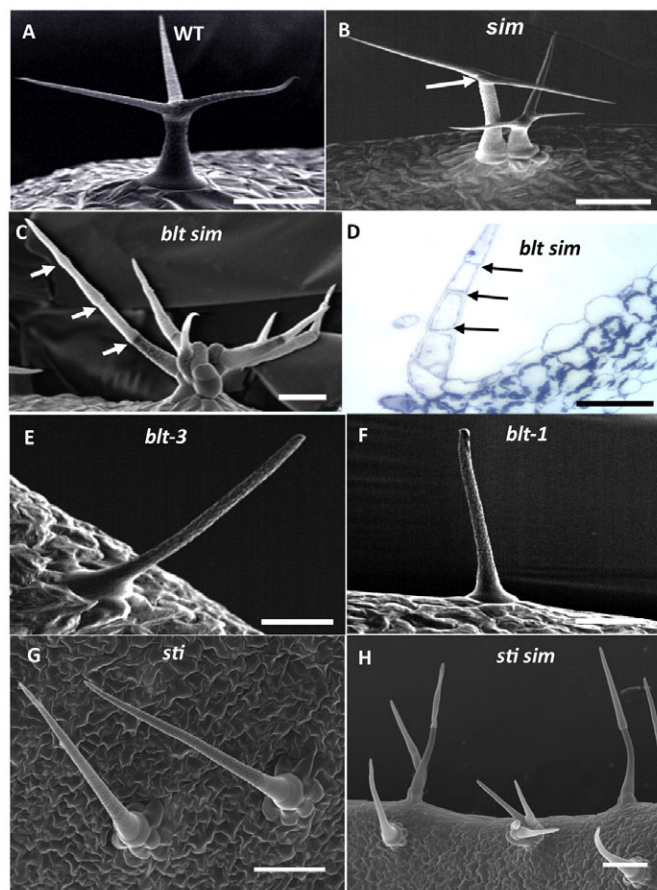


Fig. 1. Identification of a genetic enhancer of *sim* multicellular trichomes. (A-C,E-H) Scanning electron micrographs (SEMs) of (A) wild-type (WT, Col-0), (B) *sim-1*, (C) *blt-3 sim-1* double-mutant, (E) *blt-3*, (F) *blt-1*, (G) *sti-AS* and (H) *sti-AS sim* double-mutant *Arabidopsis* trichomes. Arrows indicate representative cell junctions. (D) Transverse section of a *blt-3 sim-1* double-mutant trichome stained with Toluidine Blue. Arrows indicate individual cells. Scale bars: 50 μm in A,D,H; 100 μm in B,E-G.

complexes and regulates endoreplication onset in *Arabidopsis* (Churchman et al., 2006; Peres et al., 2007). In a search for genetic modifiers of the *sim* mutant trichome phenotype, we identified a recessive mutation that greatly enhanced the multicellularity of the *sim* mutant trichome phenotype in double mutants (Fig. 1C,D; Table 1). When separated from *sim*, the single mutant of this

Table 1. *blt* increases the multicellularity of *sim* mutant trichomes

Genotype	No. of nuclei per trichome*	Total trichomes [†]
Col-0	1.0±0.0	50
<i>blt-3</i>	1.0±0.0	47
<i>sim-1</i>	2.2±1.2	64
<i>blt-3 sim-1</i>	9.8±3.3	40
<i>sti</i>	1.0±0.0	50
<i>sti sim</i>	1.2±0.5	50

The numbers of nuclei per trichome in *sim-1* versus *blt-3 sim-1* are significantly different ($P < 0.001$, Mann-Whitney rank sum test).

*The number of nuclei per trichome was counted under a fluorescence microscope (trichomes were stained with DAPI). Data are mean \pm s.d.

[†]The total number of trichomes for which nuclei were counted on first or second leaves. At least ten leaves were examined per genotype.

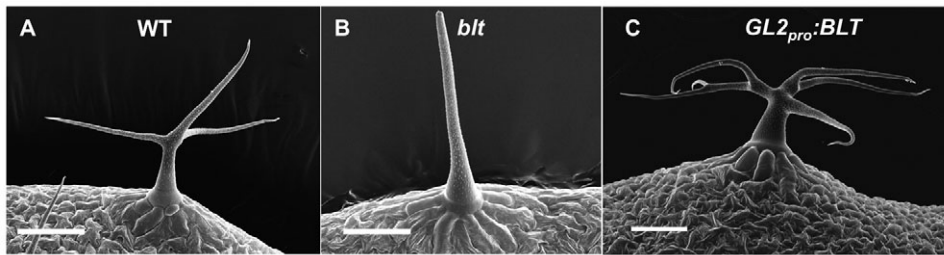


Fig. 2. *BLT* overexpression increases branching. SEMs of trichomes of (A) Col-0 wild-type, (B) *blt-3* and (C) *GL2_{pro}:BLT* in Col-0. Scale bars: 100 μ m.

modifier produces predominantly unbranched trichomes on leaves (Fig. 1E). Root growth, plant size, growth rate, floral structure and general appearance of these single mutants were identical to those of wild type, and the number of trichomes on single-mutant leaves was indistinguishable from that of wild-type leaves, indicating that the mutant phenotype is primarily or exclusively limited to post-initiation trichome development.

The unbranched trichome mutation was mapped, and sequencing of candidate genes revealed a point mutation in the gene *AT1G64690*, which has been named *BRANCHLESS TRICHOMES (BLT)* (Marks et al., 2009). The genetic modifier responsible for enhancing the *sim* phenotype was shown to be allelic to *blt* by the following criteria. First, the trichome mutant identified here produced unbranched trichomes that were phenotypically identical to those of the *blt-1* reference allele (Fig. 1F), and the two mutations failed to complement. The phenotype of our unbranched trichome allele was also completely rescued by a genomic DNA fragment containing *BLT* (see Fig. S1 in the supplementary material). Finally, when the *blt-1* reference allele was combined with either of two *sim* alleles, it produced an enhancement of the *sim* multicellular trichome phenotype identical to that seen with our initial *blt* allele (see Fig. S2 in the supplementary material). These results indicate that the gene responsible for the genetic enhancement of cell division in *sim* mutants observed in our screen was *BLT*, a gene with no known role in the cell cycle.

In accordance with the naming of *blt* alleles in previous work (Marks et al., 2009), we refer to the point-mutant allele generated in our screen as *blt-3*. This allele contains a G-to-A mutation in *AT1G64690* that changes the amino acid tryptophan (TGG) to a stop codon (TGA) at codon 64, eliminating more than 70% of the predicted protein. Thus, *blt-3* is likely to be a null allele. The *blt-3* allele was used for the studies described below unless otherwise indicated.

Loss-of-function mutations in another gene, *STI*, result in unbranched trichomes very similar in phenotype to those of the *blt* mutants (Fig. 1G) (Ilgenfritz et al., 2003). Double-mutant *sti sim* plants, however, did not exhibit an increase in the number of cells per trichome relative to *sim* trichomes (Fig. 1H; Table 1). Thus, the

dramatic enhancement of the *sim* multicellular trichome phenotype seen in *sim blt* double mutants (Fig. 1C,D; Table 1) represents a unique link between trichome branching and the cell cycle.

***BLT* represents an ancient plant protein lineage of unknown function**

The 273 amino acid product of *BLT* predicted by conceptual translation does not closely resemble any protein of known function, although sequences similar to *BLT* are found in most, if not all, angiosperm genomes (see Fig. S3 in the supplementary material). Additionally, four other *Arabidopsis* genes (*AT3G20350*, *AT1G50660*, *AT5G22310* and *AT5G22310*), all of unknown function, encode proteins that share the predicted amino acid sequence REERVQMKL (residues 161-169 of *BLT*), as well as other limited similarity with *BLT*. There is a clear and strongly supported monophyletic clade of *BLT*-related genes in all of the angiosperm species examined, indicating that the *BLT* clade originated before the last common ancestor of monocots and dicots (see Fig. S4 in the supplementary material). This suggests that *BLT* encodes an ancient conserved function, which is represented in the *Arabidopsis* genome only by *BLT* itself. Sequences with similarity to *BLT* also occur in *Physcomitrella patens* (Hedw.) Bruch & Schimp, but the sequences are from partial cDNAs and it is not possible to determine whether they represent *BLT* orthologs or paralogs.

***BLT* is a key positive regulator of trichome branching**

BLT was initially identified among a number of genes in a transcriptomics study of trichome development (Marks et al., 2009). To further investigate the role of *BLT* in trichome branching, transgenic lines expressing *BLT* from the *GL2* promoter, *GL2_{pro}*, were created. In leaves, this strong promoter drives expression predominantly in developing trichomes. Numerous transgenic lines were obtained, and most independent *GL2_{pro}:BLT* lines showed increased trichome branching (Fig. 2); counts of trichome branch points from three representative lines are shown in Table 2. Thus, when expressed from a strong trichome promoter, *BLT* expression actively promotes trichome branching.

Table 2. Plants overexpressing *BLT* have increased branching

Genotype	No. of branch points*							No. of trichomes [†]
	0	1	2	3	4	5	6	
Col-0	0.0	0.0	73.9	26.1	0.0	0.0	0.0	119
<i>blt-3</i>	87.3	12.7	0.0	0.0	0.0	0.0	0.0	106
<i>GL2_{pro}:BLT</i> line 1	0.0	0.0	25.9	30.2	29.3	12.9	1.7	116
<i>GL2_{pro}:BLT</i> line 2	0.0	0.0	32.3	36.5	23.9	7.3	0.0	96
<i>GL2_{pro}:BLT</i> line 3	0.0	1.1	30.1	43.0	22.6	3.2	0.0	93

Based on a Kruskal-Wallis one-way ANOVA on ranks and an all pairwise multiple comparison test (Dunn's Test), branch counts of all *GL2_{pro}:BLT* lines differ significantly ($P < 0.05$) from both Col-0 and *blt-3*, and branch counts of Col-0 and *blt-3* differ significantly from each other ($P < 0.05$).

*Shown in the percentage of total trichomes having the indicated number of branch points (one branch point indicates a trichome with two branches). Counts were made on first or second leaves of each genotype.

[†]Total number of trichomes on which branches were counted.

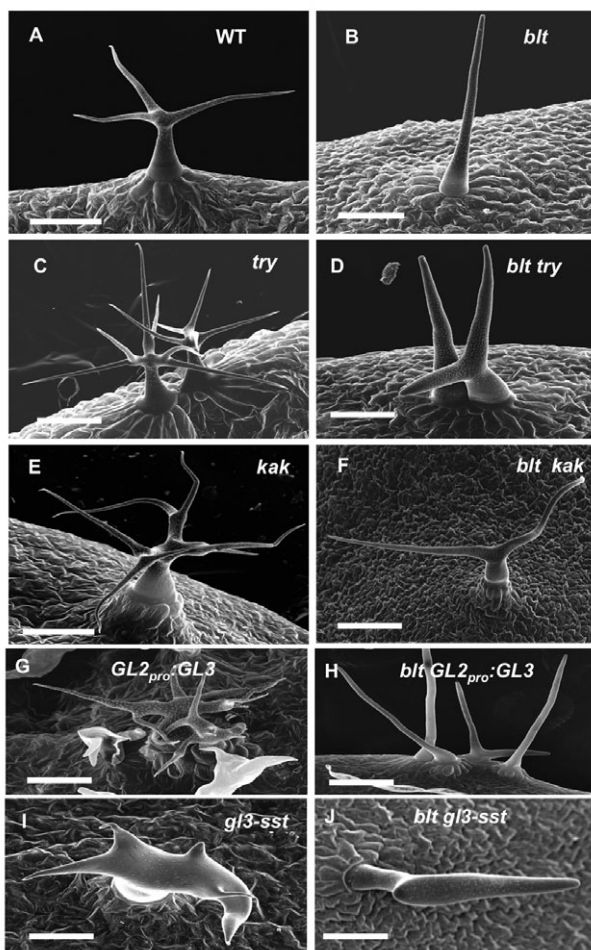


Fig. 3. *blt* is epistatic to mutations that increase trichome branching. SEMs of (A) Col-0, (B) *blt-3*, (C) *try-JC*, (D) *blt-3 try-JC*, (E) *kak-2*, (F) *blt-3 kak*, (G) *GL2_{pro}:GL3*, (H) *blt-3 GL2_{pro}:GL3*, (I) *gl3-sst* and (J) *blt-3 gl3-sst* *Arabidopsis* trichomes. Scale bars: 100 μ m.

The necessity for *BLT* function in trichome branching was also addressed by constructing double mutants between *blt* and *triptychon* (*try*), *noeck* (*nok*), *kaktus* (*kak*), *rastafari* (*rfi*), the *GL3*

gain-of-function allele *glabra3-shapeshifter* (*gl3-sst*) and the *GL3* overexpression construct *GL2_{pro}:GL3*. Each of these latter mutants and constructs produces substantial numbers of trichomes with more than four branch points (i.e. at least five branches) (Folkers et al., 1997; Perraiza et al., 1999; Esch et al., 2003). In the double mutants, the *blt* mutation greatly reduced trichome branching relative to the second mutation on its own, and very few trichomes had more than one branch point (Fig. 3; Table 3). Both *blt* alleles that we examined produced at least a few trichomes with one branch point (Table 3). Thus, *blt* is essentially epistatic to *try*, *nok*, *kak* and *rfi*. In double mutants, *blt* mutation also restricted the branching potential resulting from the *gl3-sst* gain-of-function allele or the artificially engineered *GL3* gain-of-function resulting from expression from the *GL2* promoter (Fig. 3), although owing to the complex branching pattern and trichome clustering that occur in these *GL3* gain-of-function situations it was difficult to quantitate the degree of trichome branching.

It should be noted that the sole existing *rfi* allele, as used here, contains a C-to-T point mutation in the *GL3* gene that converts codon 116 from GCC (Ala) to GTC (Val). This *rfi* allele maps close to *gl3* on chromosome five. Thus, *rfi* might be another *gl3* gain-of-function mutation.

***BLT* couples cellular morphogenesis and endoreplication in trichomes**

In many, but not all, cases, a positive correlation exists between the average number of trichome branches associated with a particular genotype and the degree of endoreplication of trichome nuclear DNA (Hülkamp et al., 1994; Larkin et al., 2007). One mutant that does not show such a correlation is *sti*; trichomes of *sti* mutant plants have little branching, but have a nuclear DNA content similar to that of wild type (Ilgenfritz et al., 2003). Similarly, we found that *blt* mutation had no effect on trichome nuclear DNA content (Fig. 4A) or on the nuclear DNA content of leaf cells (Fig. 4B). These results indicate that, like *STI*, *BLT* function is not required for endoreplication. However, three *GL2_{pro}:BLT* overexpression lines all showed a significant increase in DNA content relative to wild-type or *blt* mutant trichomes (Fig. 4C). This result suggested that *BLT* function is necessary to couple trichome branching to the degree of endoreplication. To test this hypothesis, we examined the nuclear DNA content of *blt gl3-sst* and *blt try* double mutants in comparison to the respective single mutants, *gl3-*

Table 3. Loss of *BLT* function limits branching potential in double mutants

Genotype	No. of branch points*								No. of trichomes [†]
	0	1	2	3	4	5	6	7	
Col-0	0.0	0.0	93.4	6.6	0.0	0.0	0.0	0.0	244
<i>blt-3</i>	82.9	17.1	0.0	0.0	0.0	0.0	0.0	0.0	258
<i>try-JC</i>	0.0	0.0	1.3	11.5	36.5	36.2	12.2	2.3	304
<i>blt-3 try-JC</i>	55.7	37.8	6.5	0.0	0.0	0.0	0.0	0.0	246
<i>kak-2</i>	0.0	0.0	0.6	14.5	33.0	35.8	11.7	4.3	324
<i>blt-3 kak-2</i>	16.9	83.1	0.0	0.0	0.0	0.0	0.0	0.0	242
<i>nok</i>	0.0	1.5	26.1	50.7	20.1	1.5	0.0	0.0	134
<i>blt nok</i>	34.3	65.1	0.6	0.0	0.0	0.0	0.0	0.0	169
<i>rfi</i>	0.0	0.0	0.4	21.3	36.8	31.6	7.6	2.2	225
<i>blt-3 rfi</i>	56.4	43.3	0.3	0.0	0.0	0.0	0.0	0.0	307
<i>gl3-1</i>	63.2	33.5	3.2	0.0	0.0	0.0	0.0	0.0	151
<i>blt-3 gl3-1</i>	97.7	2.3	0.0	0.0	0.0	0.0	0.0	0.0	299

For each comparison of a single trichome branching mutant with its double mutant with *blt-3*, as well as for the comparison of Col-0 with *blt-3*, the median number of branch points per trichome differed significantly ($P < 0.001$) based on a Mann-Whitney rank sum test.

*Shown is the percentage of trichomes having the indicated number of branch points (one branch point indicates a trichome with two branches). Counts were made on ten first or second leaves per genotype.

[†]Total number of trichomes on which branches were counted.

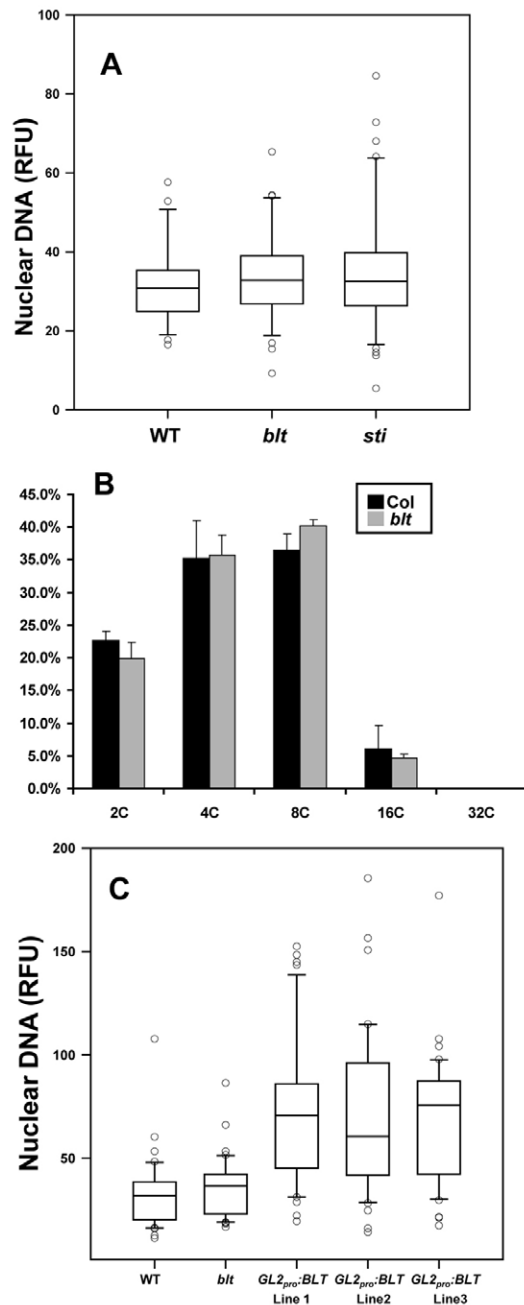


Fig. 4. *BLT* overexpression increases nuclear DNA content. (A) In situ measurements of trichome nuclear DNA content of *blt-3* and *sti-AS* loss-of-function mutants. Relative fluorescence units (RFU) have been normalized to approximately correspond to haploid genome equivalents (C values). None of the pairwise comparisons among these three genotypes is significant [$P > 0.05$, Kruskal-Wallis one-way ANOVA on ranks and an all pairwise multiple comparison test (Dunn's test)]. (B) Nuclear DNA content of 21-day-old wild-type (Col) and *blt* *Arabidopsis* leaves, as determined by flow cytometry. The percentage of nuclei in each ploidy class is indicated. Error bars indicate s.d. (C) In situ measurements of trichome nuclear DNA content of *GL2_{pro}:BLT* overexpression lines. All three *GL2_{pro}:BLT* lines differ significantly from wild type and *blt* ($P < 0.05$, Kruskal-Wallis one-way ANOVA on ranks and Dunn's test). Data in A and C are presented as box plots, in which the box encompasses the 25th through to the 75th percentile of the data, the line within the box is the median (50th percentile), and the error bars represent the 5th (lower bar) and the 95th (upper bar) percentiles.

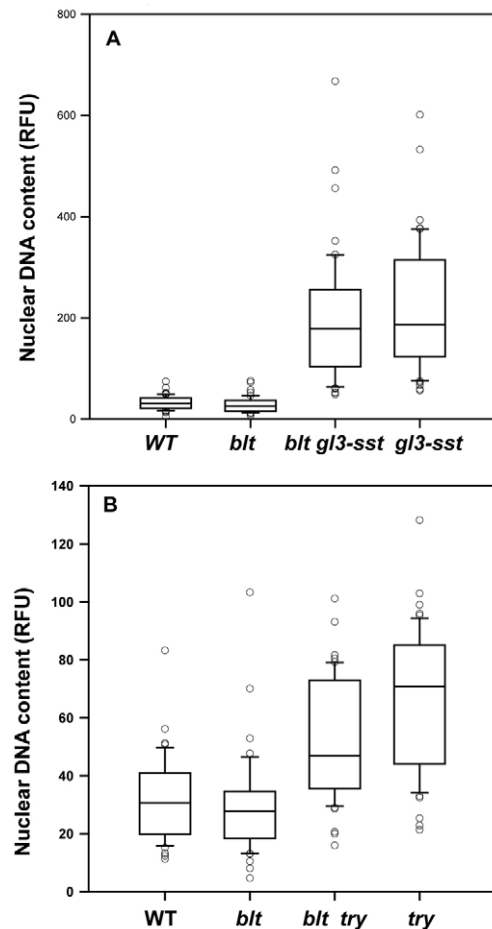


Fig. 5. Loss of *BLT* function uncouples DNA content from morphogenesis in increased branching mutants. (A) Comparison of *gl3-sst* and *blt-3 gl3-sst* DNA contents. Based on a Kruskal-Wallis one-way ANOVA on ranks and Dunn's test, all pairwise comparisons differ significantly ($P < 0.05$), except for *gl3-sst* versus *blt-3 gl3-sst* and for wild type versus *blt*. (B) Comparison of *try* and *blt-3 try*. In a Kruskal-Wallis one-way ANOVA on ranks and Dunn's test, all pairwise comparisons differ significantly ($P < 0.05$), except for *try-JC* versus *blt try-JC* and for wild type versus *blt*. Box plot data are presented as described in Fig. 4. RFU are normalized to approximately correspond to haploid genome equivalents (C values).

sst and *try*, both of which result in increased branching and nuclear DNA content on their own. Both double mutants exhibited an elevated DNA content that was not significantly different from that of the corresponding single mutant (Fig. 5A,B), even though *blt* substantially restricts branching in the double mutants (Fig. 3D,J; Table 3). This was particularly striking for the *gl3-sst* allele. Although it was difficult to accurately count the number of branches on trichomes of plants homozygous for this *gl3* gain-of-function allele owing to highly variable branch expansion and trichome shape, it was clear that *gl3-sst* single mutants have an increased number of branch points per trichome, and trichomes having greater than four branch points were common (Fig. 3I) (Esch et al., 2003). In spite of an obvious and dramatic reduction of branching in *blt gl3-sst* trichomes (Fig. 3J), these trichomes had a median DNA content that was more than fourfold higher than that of wild type and indistinguishable from that of *gl3-sst* single-mutant trichomes (Fig. 4A).

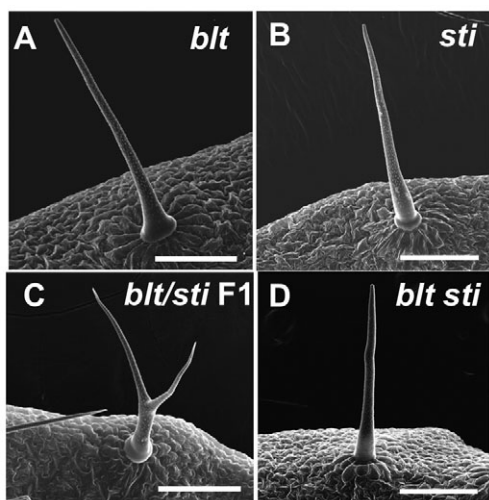


Fig. 6. Partial intergenic non-complementation between *blt* and *sti*. SEMs of (A) *blt-3*, (B) *sti-AS*, (C) *blt-3/+ sti-AS/+* F1 and (D) *blt-3 sti-AS* homozygous double-mutant *Arabidopsis* trichomes. Scale bars: 100 μ m.

In a separate experiment, we found that, whereas individual *sim* nuclei had a mean DNA content of 12.4 ± 7.3 relative fluorescence units (RFU), individual *blt sim* nuclei had a mean DNA content of 3.1 ± 3.3 RFU. The DNA content of *blt sim* nuclei was significantly different from that of both *sim* and *blt* [$P < 0.05$, Kruskal-Wallis one-way ANOVA on ranks and an all pairwise multiple comparison test (Dunn's test)]. When these data were combined with the number of nuclei per trichome initiation site for each genotype (Table 1), the total nuclear DNA content per trichome initiation site was similar in the two genotypes (27.2 RFU for *sim* and 30.4 for *blt sim*). Thus, in the *blt sim* double-mutant combination, *blt* increases mitotic divisions above the degree of division seen in the *sim* single mutant, without affecting the number of cycles of DNA replication.

We also considered the hypothesis that, although *blt* mutations do not affect the level of endoreplication reached by mature trichomes, they might prolong a juvenile developmental stage permissive for division, in which case we might see an alteration in the timing of endoreplication in early stages of *blt* trichome development. It is difficult to obtain accurate in situ DNA content values from early trichome developmental stages owing to the high background and close spacing of cells. Therefore, as a proxy for

endoreplication in early trichome development stages, we used the widest cross-sectional area of stage one and stage two trichome nuclei, i.e. the nuclei of trichomes that are less than twice as tall as they are wide, prior to the initiation of branching in wild-type trichomes (Szymanski et al., 1998). The nuclei of surrounding protodermal cells, which were still dividing, were also examined. Because the nuclei of these cells appear to be essentially spherical, this cross-sectional area should be indicative of cell volume (Walker et al., 2000). No difference was found between wild-type and *blt* nuclei for early-stage developing trichomes or dividing protodermal cells (see Table S1 in the supplementary material), indicating that there is no obvious alteration in the timing of endoreplication in the early development of *blt* trichomes.

BLT interacts both genetically and physically with STI, another positive regulator of trichome branching

Mutations in only two genes, *blt* and *sti*, result in trichomes that are unbranched but otherwise develop normally. As noted by Marks et al. (Marks et al., 2009), *blt sti* double mutants resemble the two parental mutants, a result that is consistent with the two gene products acting in the same pathway. However, in constructing this double mutant, we noticed that 25-30% of the trichomes on F1 plants heterozygous for both *blt* and *sti* had only a single branch point (i.e. were two-branched; Fig. 6; Table 4), a phenotype that is almost never seen in the Col-0 wild-type background in which both mutations were derived, and is rare (less than 3%) in F1 heterozygotes between either *blt* or *sti* and wild type. Thus, *blt* and *sti* exhibit substantial intergenic non-complementation.

Intergenic non-complementation is often observed in cases in which two protein products act as part of the same complex (Huffaker et al., 1987). We tested the hypothesis that the BLT and STI proteins interact using two methods. Yeast two-hybrid experiments demonstrated a clear interaction between the N-terminal 472 amino acids of STI and full-length BLT (Fig. 7A-D; Table 5). Interaction between STI and BLT was confirmed by in planta bimolecular fluorescence complementation (BiFC) experiments in which full-length *STI* and *BLT* coding regions were respectively fused to the N-terminal and C-terminal split domains of YFP and co-bombarded into onion cells, which resulted in YFP fluorescence indicative of close association of the two test proteins (Fig. 7E,F).

We also investigated the localization of BLT and STI fluorescent protein fusions in developing trichomes of *sti* and *blt* mutants, respectively, using transient expression of YFP fusions introduced into developing trichomes via biolistic bombardment of developing

Table 4. Genetic interaction between *blt* and *sti* for trichome branching phenotype

Genotype	No. of branch points*					No. of trichomes [†]
	0	1	2	3	4	
Col-0	0.0	0.0	78.0	12.8	0.2	392
<i>blt-3</i>	90.7	9.3	0.0	0.0	0.0	236
<i>sti-AS</i>	99.7	0.3	0.0	0.0	0.0	292
Col-0 \times <i>blt-3</i> F1 (heterozygote)	0.0	2.7	97.3	0.0	0.0	480
Col-0 \times <i>sti-AS</i> F1 (heterozygote)	0.0	2.8	96.8	0.4	0.0	497
<i>blt-3</i> \times <i>sti-AS</i> F1 (heterozygote)	0.0	31.3	68.7	0.0	0.0	399
<i>blt-3 sti-AS</i>	100.0	0.0	0.0	0.0	0.0	368

Based on a Kruskal-Wallis one-way ANOVA on ranks and an all pairwise multiple comparison test (Dunn's test), branch counts of *blt-3* \times *sti-AS* F1 trichomes differed significantly ($P < 0.05$) from both Col-0 \times *blt-3* F1 trichomes and Col-0 \times *sti-AS* F1 trichomes, whereas Col-0 \times *sti-AS* F1 trichomes and Col-0 \times *sti-AS* F1 trichomes did not differ significantly.

*Shown is the percentage of trichomes having the indicated number of branch points (one branch point indicates a trichome with two branches). Counts were made on ten first or second leaves per genotype.

[†]Total number of trichomes on which branches were counted.

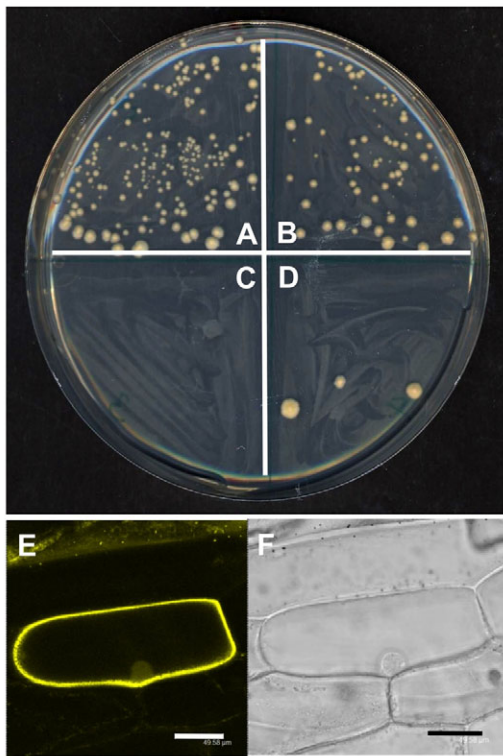


Fig. 7. Interaction between BLT and STI in yeast two-hybrid and BiFC assays. (A–D) Yeast two-hybrid interaction of BLT with a domain of STI that comprises the N-terminal 454 amino acids. Yeast strain AH109 cells co-expressing bait and prey plasmids were allowed to grow on $-Trp/-Leu$ plates and then on $-Trp/-Leu/-His+3AT$ to test for protein-protein interaction. (A) *pBD-STI N-term/pAD-BLT*, (B) *pBD-SNF1/pAD-SNF4* (positive control), (C) *pBD-STI N-term/pAD-GUS* (negative control) and (D) *pBD-GUS/pAD-BLT* (negative control). (E) Confocal image of interaction between BLT and STICHEL (STI) using BiFC. *BLT* and *STI* fused with the C-terminal and N-terminal split fragments of YFP, respectively, were co-bombarded into onion cells. The YFP fluorescence (yellow) from the BiFC complex serves as an indicator of the interaction between BLT and STI proteins. When both fusion clones were co-bombarded, 20–30 YFP-positive cells were observed in each of four independent experiments. No YFP-positive cells were observed when either fusion was bombarded individually, or in bombardments with empty vector. (F) Phase-contrast image of the cell shown in E. Scale bars: 50 μ m.

leaves (Fig. 8). In all *sti* early-stage trichomes expressing YFP:BLT, YFP fluorescence was localized apically, similar to the YFP:BLT localization seen in wild type (Fig. 8A,B). Twelve of fifteen *blt* cells expressing STI:YFP also exhibited the apical localization observed for STI:YFP in wild type (Fig. 8C,D), whereas three cells exhibited

a more lateral localization of the fluorescent signal not seen in wild-type controls. No trichomes in either experiment showed detectable nuclear-localized fluorescence.

DISCUSSION

In most genotypes, the degree of endoreplication is highly correlated with trichome branching (Hülkamp et al., 1994; Larkin et al., 2007), but the mechanism that maintains this correlation is unknown. The cell polarity mechanism involved in trichome branch initiation is likewise poorly understood. Here, we have found that the product of the *BLT* gene, previously known as a regulator of trichome branch initiation (Marks et al., 2009), can also influence the cell cycle in developing trichomes. This suggests that BLT is a component of the mechanism that coordinates branch initiation and the endoreplication cell cycle in developing trichomes.

The *BLT* gene is unique in the *Arabidopsis* genome, with the most closely related *Arabidopsis* genes clearly being paralogs (see Fig. S3 in the supplementary material). Both monocots and dicots have *BLT* homologs (see Fig. S3 in the supplementary material), indicating that the function of the gene product has been conserved throughout angiosperm evolution, although neither BLT nor its paralogs resemble any genes of known function. Marks et al. predicted that the BLT protein sequence has a high probability of adopting a coiled-coil structure throughout much of its length (Marks et al., 2009). Based on data collated at the Genevestigator website (Hruz et al., 2008), *BLT* is widely expressed in *Arabidopsis*, with the highest levels seen in testa, the root hair zone and petals. The transcriptional pathways that control mucilage formation in the testa and root epidermal fate share transcription factors with the trichome cell fate pathway. However, we detected no defects in mucilage formation or root hair development in *blt* mutants (our unpublished observations).

Overexpression of *BLT* resulted in the initiation of supernumerary branches (Fig. 2; Table 2). In double-mutant combinations with increased trichome branching mutants, a *blt* mutation severely restricted branching and was essentially epistatic to the increased branching mutant in each case (Fig. 3; Table 3). Thus, *BLT* function is essential for branching, and, when overexpressed in wild type, *BLT* is sufficient to promote branch initiation, properties that are expected of a major regulator of branch initiation. These results significantly strengthen the evidence indicating that *BLT* plays a key role in trichome branch initiation.

Perhaps most significantly, the work presented here indicates that BLT forms a protein complex with STI, another protein directly involved in branch initiation. Four lines of evidence support this conclusion. First, F1 heterozygotes resulting from crosses between *blt* and *sti* show a degree of intergenic non-complementation for branching, producing significant numbers of two-branched trichomes (trichomes with a single branch point; Fig. 6C), whereas the wild type and either individual mutant

Table 5. Yeast two-hybrid screen for interaction of BLT with STICHEL

Bait	Prey	mM 3AT				α -galactosidase [†]	n
		0	3	5	10		
STI-N term	BLT	+	+	+	+	1.7 \pm 0.3	6
STI-N term	GFP*	+	–	–	–	0.1 \pm 0.1	6
GFP*	BLT	–	–	–	–	0 \pm 0	6

A *t*-test indicated that the α -galactosidase activity resulting from the STI-N term/BLT combination differed significantly from that of the STI-N term/GFP negative control combination ($P < 1 \times 10^{-6}$).

+, Positive interaction; –, no interaction. 3AT, 3-amino-1,2,4-triazole.

*, Negative control.

[†]Milliunits of α -galactosidase activity $\text{ml}^{-1} \text{cell}^{-1}$. α -galactosidase activity results from expression of the GAL4-responsive *MEL1* reporter present in the AH109 host strain. Six independent colonies of each genotype were assayed for α -galactosidase activity.

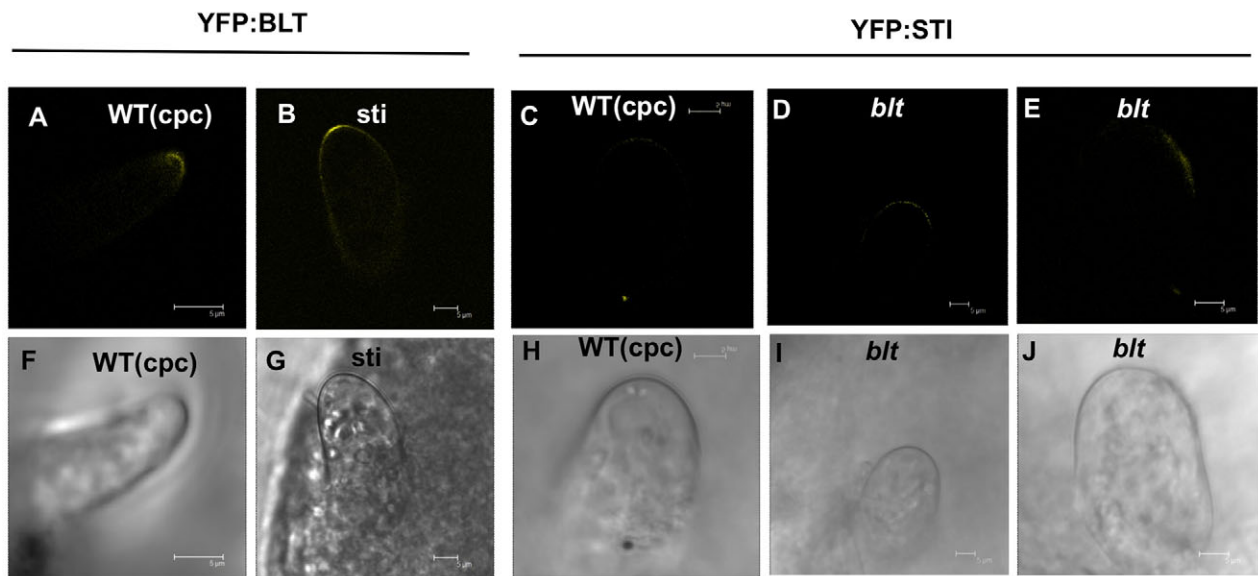


Fig. 8. Localization of YFP:BLT in *sti* and of STI:YFP in *blt* by transient expression in biologically transformed developing trichomes. (A–J) To reduce the total number of bombardments needed, *cpc* mutant plants, which have an increased number of trichomes on leaves, were used as the wild-type control. Preliminary experiments demonstrated that *CPC* and *cpc* plants exhibit an identical apical localization of YFP:BLT and STI:YFP. YFP fluorescence (A–E) and bright-field (F–J) images are shown for each of the developing trichomes. Scale bars: 5 μ m.

heterozygote produce predominately three-branched trichomes (trichomes with two branch points) and very few two-branched trichomes (Table 4). Such intergenic non-complementation is often observed between components of a protein complex; examples include yeast (Huffaker et al., 1988) and *Drosophila* (Hays et al., 1989) α - and β -tubulin, components of a yeast G-protein signaling cascade (Akada et al., 1996), and the trichome cell fate transcription complex in *Arabidopsis* (Larkin et al., 1999). Second, full-length BLT interacted strongly with the N-terminal domain of STI in a yeast two-hybrid assay (Fig. 7A; Table 5), although interaction between BLT and full-length STI was at best weak (our unpublished observations). Third, full-length BLT and full-length STI interact in BiFC assays in living onion epidermal cells (Fig. 7E). Finally, Marks et al. have shown that biologically functional fluorescent protein fusions of both BLT and STI co-localize in developing trichome branch tips (Marks et al., 2009).

Taken together with the gain-of-function and loss-of-function phenotypes of *blt* and *sti*, these results make a strong case for a protein complex that contains both BLT and STI functioning as a key polarity determinant in trichome branch initiation. As with BLT, little functional information for the STI protein can be inferred from its protein sequence. STI has sequence similarity to eubacterial DNA polymerase III γ -subunits (Ilgenfritz et al., 2003), but given that *sti* mutants have no effect on DNA replication and that it appears to be localized in the cytoplasm, at the branch tips, the significance of this similarity is unclear. Nonetheless, the identification of a protein complex involved in branch initiation opens up new avenues to an understanding of cell shape using the trichome model. The primary role of BLT would thus seem to be at the branch initiation sites in a complex with STI. Not only do the proteins interact, but the effects on trichome branch initiation of manipulating *BLT* or *STI* function are identical: loss-of-function mutations in either gene virtually eliminate branching, whereas overexpression of either gene results in increased branching. By contrast, only manipulation of *BLT* function affects endoreplication: *BLT* overexpression

increases trichome nuclear DNA content (Fig. 4C), whereas *STI* overexpression has no effect on DNA content (Ilgenfritz et al., 2003).

Our data suggest that, in addition to its role in promoting branch formation, BLT functions in a signaling mechanism that originates at the branch tips and maintains homeostasis between the number of branches and nuclear DNA content. Given that *blt* loss-of-function mutants do not exhibit reduced endoreplication, BLT is presumably not directly necessary for endoreplication, but functions to increase endoreplication to ‘catch up’ if branching increases faster than DNA content. Excess free BLT that is not localized to branch points does not appear to be the signaling molecule as nuclear BLT has not been detected, and YFP:BLT is not detectably mislocalized in developing *sti* mutant trichomes (Fig. 8). We also found that, although *blt* mutations increase cell division in combination with *sim* (Fig. 1C,D; Table 1), *blt sim* mutant trichome initiation sites have the same total DNA content for all nuclei as *sim* trichome initiation sites, indicating again that *blt* loss-of-function has no effect on the number of rounds of DNA replication. Thus, BLT must also have a minor second function in suppressing mitosis in trichomes that is revealed only when the primary mitosis-suppressing function is compromised by a *sim* mutation.

A candidate nuclear target of such a signaling pathway linking branching and endoreplication is Chromatin assembly factor-1 (CAF-1), which is involved in the replication-dependent deposition of histones H3 and H4 onto DNA (Groth et al., 2007). Mutations in CAF-1 subunits result in trichomes with increased branching but normal endoreplication (Exner et al., 2006). Mutations in *sti* are epistatic to mutations affecting two different CAF-1 subunits, and CAF-1 function is necessary for the extra endoreplication cycles that result from *kak* mutations (Exner et al., 2008). CAF-1 thus resembles BLT in having a primary role in trichome branching and a more cryptic role in endoreplication. Several cell fate transcription factors affect the degree of endoreplication when mutated or overexpressed (Larkin et al., 2007), and these constitute other possible nuclear targets of such a pathway.

The results presented here provide insight into the coordination of cell shape and DNA content in an endoreplicating cell, as well as advancing our understanding of a protein complex that is involved in specifying cell shape. It has previously been speculated that trichome branching mechanisms were derived from the cell division machinery (Schnittger and Hülskamp, 2002). Although our results do not directly support this idea, the work presented here opens new avenues for investigating the relationship between cell shape, cell differentiation and the cell cycle.

Acknowledgements

We thank Dr Arp Schnittger and Dr Alan Wolfe and the Advanced Genetics students at Loyola University Health System in Fall 2008 for critical comments and useful discussions; Lieven De Veylder for the flow cytometry data in Fig. 4B; Jean-Marc Bonneville, M. David Marks and Alan Sessions for the gift of seed stocks; and TAIR and the Arabidopsis Biological Resource Center for database information, seeds and DNA stocks. Funding for this work was provided by an NSF grant (IOS 0744566) to J.C.L. and a DFG grant (SPP 1111) to M.H. C.-C.H. was supported by the International Graduate School.

Competing interests statement

The authors declare no competing financial interests.

Supplementary material

Supplementary material for this article is available at <http://dev.biologists.org/lookup/suppl/doi:10.1242/dev.058982/-DC1>

References

- Abrash, E. B. and Bergmann, D. C.** (2009). Asymmetric cell divisions: a view from plant development. *Dev. Cell* **16**, 783-796.
- Aho, S., Arffman, A., Pummi, T. and Uitto, J.** (1997). A novel reporter gene MEL1 for the yeast two-hybrid system. *Anal. Biochem.* **253**, 270-272.
- Akada, R., Kallal, L., Johnson, D. I. and Kurjan, J.** (1996). Genetic relationships between the G-protein β complex, Ste5p, Ste20p, and Cdc42p: investigation of effector roles in the yeast pheromone response pathway. *Genetics* **143**, 103-117.
- Bouyer, D., Geier, F., Kragler, F., Schnittger, A., Pesch, M., Wester, K., Balkunde, R., Timmer, J., Fleck, C. and Hülskamp, M.** (2008). Two-dimensional patterning by a trapping/depletion mechanism: the role of TTG1 and GL3 in Arabidopsis trichome formation. *PLoS Biol.* **6**, e141.
- Castellano, M. M., Boniotti, M. B., Caro, E., Schnittger, A. and Gutierrez, C.** (2004). DNA replication licensing affects cell proliferation or endoreplication in a cell type-specific manner. *Plant Cell* **16**, 2380-2393.
- Churchman, M. L., Brown, M. L., Kato, N., Kirik, V., Hülskamp, M., Inze, D., De Veylder, L., Walker, J. D., Zheng, Z., Oppenheimer, D. G. et al.** (2006). SIAMESE, a plant-specific cell cycle regulator, controls endoreplication onset in Arabidopsis thaliana. *Plant Cell* **18**, 3145-3157.
- Clough, S. J. and Bent, A. F.** (1998). Floral dip: a simplified method for *Agrobacterium*-mediated transformation of *Arabidopsis thaliana*. *Plant J.* **16**, 735-743.
- Desvoyes, B., Ramirez-Parra, E., Xie, Q., Chua, N. H. and Gutierrez, C.** (2006). Cell type-specific role of the retinoblastoma/E2F pathway during Arabidopsis leaf development. *Plant Physiol.* **140**, 67-80.
- Esch, J. J., Chen, M., Sanders, M., Hillestad, M., Ndkium, S., Idelkopo, B., Neizer, J. and Marks, M. D.** (2003). A contradictory GLABRA3 allele helps define gene interactions controlling trichome development in Arabidopsis. *Development* **130**, 5885-5894.
- Exner, V., Taranto, P., Schonrock, N., Gruitsem, W. and Hennig, L.** (2006). Chromatin assembly factor CAF-1 is required for cellular differentiation during plant development. *Development* **133**, 4163-4172.
- Exner, V., Gruitsem, W. and Hennig, L.** (2008). Control of trichome branching by chromatin assembly factor-1. *BMC Plant Biol.* **8**, 54.
- Folkers, U., Berger, J. and Hülskamp, M.** (1997). Cell morphogenesis of trichomes in Arabidopsis: differential control of primary and secondary branching by branch initiation regulators and cell growth. *Development* **124**, 3779-3786.
- Groth, A., Rocha, W., Verreault, A. and Almouzni, G.** (2007). Chromatin challenges during DNA replication and repair. *Cell* **128**, 721-733.
- Hays, T. S., Deuring, R., Robertson, B., Prout, M. and Fuller, M. T.** (1989). Interacting proteins identified by genetic interactions: a missense mutation in alpha-tubulin fails to complement alleles of the testis-specific beta-tubulin gene of *Drosophila melanogaster*. *Mol. Cell. Biol.* **9**, 875-884.
- Hruz, T., Laule, O., Szabo, G., Wessendorp, F., Bleuler, S., Oertle, L., Widmayer, P., Gruitsem, W. and Zimmermann, P.** (2008). Genevestigator v3: a reference expression database for the meta-analysis of transcriptomes. *Adv. Bioinformatics* **2008**, 420747.
- Huffaker, T. C., Hoyt, M. A. and Botstein, D.** (1987). Genetic analysis of the yeast cytoskeleton. *Annu. Rev. Genet.* **21**, 259-284.
- Huffaker, T. C., Thomas, J. H. and Botstein, D.** (1988). Diverse effects of beta-tubulin mutations on microtubule formation and function. *J. Cell Biol.* **106**, 1997-2010.
- Hülskamp, M., Miséra, S. and Jürgens, G.** (1994). Genetic dissection of trichome cell development in Arabidopsis. *Cell* **76**, 555-566.
- Ilgenfritz, H., Bouyer, D., Schnittger, A., Mathur, J., Kirik, V., Schwab, B., Chua, N. H., Jürgens, G. and Hülskamp, M.** (2003). The Arabidopsis STICHEL gene is a regulator of trichome branch number and encodes a novel protein. *Plant Physiol.* **131**, 643-655.
- Kasili, R., Walker, J. D., Simmons, L. A., Zhou, J., De Veylder, L. and Larkin, J. C.** (2010). SIAMESE cooperates with the CDH1-like protein CCS52A1 to establish endoreplication in Arabidopsis thaliana trichomes. *Genetics* **185**, 257-268.
- Kirik, V., Schnittger, A., Radchuk, V., Adler, K., Hülskamp, M. and Baumlein, H.** (2001). Ectopic expression of the Arabidopsis AtMYB23 gene induces differentiation of trichome cells. *Dev. Biol.* **235**, 366-377.
- Larkin, J., Walker, J., Bolognesi-Winfield, A., Gray, J. and Walker, A.** (1999). Allele-specific interactions between *ttg* and *gl1* during trichome development in *Arabidopsis thaliana*. *Genetics* **151**, 1591-1604.
- Larkin, J. C., Brown, M. L. and Churchman, M. L.** (2007). Insights into the endocycle from trichome development. In *Cell Cycle Control and Plant Development* (ed. D. Inzé), pp. 249-268. Oxford: Blackwell.
- Lukowitz, W., Gillmor, C. S. and Scheible, W. R.** (2000). Positional cloning in Arabidopsis. Why it feels good to have a genome initiative working for you. *Plant Physiol.* **123**, 795-805.
- Marks, M. D., Wenger, J. P., Gilding, E., Jilk, R. and Dixon, R. A.** (2009). Transcriptome analysis of Arabidopsis wild-type and *gl3-sst* sim trichomes identifies four additional genes required for trichome development. *Mol. Plant* **2**, 803-822.
- Melaragno, J., Mehrota, B. and Coleman, A.** (1993). Relationship between endoploidy and cell size in epidermal tissue of Arabidopsis. *Plant Cell* **5**, 1661-1668.
- Perazza, D., Herzog, M., Hülskamp, M., Brown, S., Dorne, A. M. and Bonneville, J. M.** (1999). Trichome cell growth in Arabidopsis thaliana can be derepressed by mutations in at least five genes. *Genetics* **152**, 461-476.
- Peres, A., Churchman, M. L., Hariharan, S., Himanen, K., Verkest, A., Vandepoole, K., Magyar, Z., Hatzfeld, Y., Van Der Schueren, E., Beemster, G. T. et al.** (2007). Novel plant-specific cyclin-dependent kinase inhibitors induced by biotic and abiotic stresses. *J. Biol. Chem.* **282**, 25588-25596.
- Pesch, M. and Hülskamp, M.** (2009). One, two, three...models for trichome patterning in Arabidopsis? *Curr. Opin. Plant Biol.* **12**, 587-592.
- Schellmann, S. and Hülskamp, M.** (2005). Epidermal differentiation: trichomes in Arabidopsis as a model system. *Int. J. Dev. Biol.* **49**, 579-584.
- Schellmann, S., Schnittger, A., Kirik, V., Wada, T., Okada, K., Beermann, A., Thumfahrt, J., Jürgens, G. and Hülskamp, M.** (2002). TRIPTYCHON and CAPRICE mediate lateral inhibition during trichome and root hair patterning in Arabidopsis. *EMBO J.* **21**, 5036-5046.
- Schnittger, A. and Hülskamp, M.** (2002). Trichome morphogenesis: a cell-cycle perspective. *Philos. Trans. R. Soc. Lond. B* **357**, 823-826.
- Smith, L. G. and Oppenheimer, D. G.** (2005). Spatial control of cell expansion by the plant cytoskeleton. *Annu. Rev. Cell Dev. Biol.* **21**, 271-295.
- Szymanski, D. B.** (2009). Plant cells taking shape: new insights into cytoplasmic control. *Curr. Opin. Plant Biol.* **12**, 735-744.
- Szymanski, D. B. and Cosgrove, D. J.** (2009). Dynamic coordination of cytoskeletal and cell wall systems during plant cell morphogenesis. *Curr. Biol.* **19**, R800-R811.
- Szymanski, D. B., Jilk, R. A., Pollock, S. M. and Marks, M. D.** (1998). Control of *GL2* expression in Arabidopsis leaves and trichomes. *Development* **125**, 1161-1171.
- Uhrig, J. F., Mutondo, M., Zimmermann, I., Deeks, M. J., Machesky, L. M., Thomas, P., Uhrig, S., Rambke, C., Hussey, P. J. and Hülskamp, M.** (2007). The role of Arabidopsis SCAR genes in ARP2-ARP3-dependent cell morphogenesis. *Development* **134**, 967-977.
- Verkest, A., Manes, C. L., Vercauysse, S., Maes, S., Van Der Schueren, E., Beeckman, T., Genschik, P., Kuiper, M., Inze, D. and De Veylder, L.** (2005a). The cyclin-dependent kinase inhibitor KRP2 controls the onset of the endoreduplication cycle during Arabidopsis leaf development through inhibition of mitotic CDKA;1 kinase complexes. *Plant Cell* **17**, 1723-1736.
- Verkest, A., Weinel, C., Inze, D., De Veylder, L. and Schnittger, A.** (2005b). Switching the cell cycle. Kip-related proteins in plant cell cycle control. *Plant Physiol.* **139**, 1099-1106.
- Vlieghe, K., Inzé, D. and De Veylder, L.** (2007). Physiological relevance and molecular control of the endocycle in plants. In *Cell Cycle Control and Plant Development* (ed. D. Inzé), pp. 227-248. Oxford: Blackwell.
- Walker, J. D., Oppenheimer, D. G., Conciene, J. and Larkin, J. C.** (2000). SIAMESE, a gene controlling the endoreduplication cell cycle in Arabidopsis thaliana trichomes. *Development* **127**, 3931-3940.
- Weigel, D. and Glazebrook, J.** (2002). *Arabidopsis: A Laboratory Manual*. Woodbury, NY: Cold Spring Harbor Laboratory Press.
- Weinel, C., Marquardt, S., Kuijt, S. J., Nowack, M. K., Jakoby, M. J., Hülskamp, M. and Schnittger, A.** (2005). Novel functions of plant cyclin-dependent kinase inhibitors, ICK1/KRP1, can act non-cell-autonomously and inhibit entry into mitosis. *Plant Cell* **17**, 1704-1722.
- Yang, Z.** (2008). Cell polarity signaling in Arabidopsis. *Annu. Rev. Cell Dev. Biol.* **24**, 551-575.